Study on the composition, microstructure, and technological orientation for the fabrication of piezoelectric ceramics used in special transducers for underwater acoustics

Trieu Khuong*, Ngo Minh Tien, Tran Van Cuong, Ha Quoc Bang

Institute of Materials, Biology and Environment, Academy of Military Science and Technology, 17 Hoang Sam, Nghia Do, Hanoi, Vietnam.
*Corresponding author: trieukhuong1504@gmail.com
Received 15 Aug. 2025; Revised 2 Oct. 2025; Accepted 16 Oct. 2025; Published 18 Nov. 2025.
DOI: https://doi.org/10.54939/1859-1043.j.mst.IMBE.2025.8-14

ABSTRACT

The paper presents research results on the composition and microstructure of piezoelectric ceramics currently used in transducers. Based on these results, a technological approach is proposed for fabricating disk-shaped piezoelectric ceramics intended for the 1H antenna of the MGK-400EM sonar system. The results show that the piezoelectric ceramic is lead-based, with an apparent density of 7.378 g/cm³, surfaces are coated with Ag, with an average thickness of 17.07 µm. The ceramic matrix consists of fine, uniform grains with an average size of ~5 µm. The EDX analysis results show that the main elements are homogeneous distributed by weight are 43.29% Pb, 10.53% Ba, 16.59% Zr, 5.87% Ti, 22.87% O, and 0.85% Sr. In this system, Sr acts as a dopant equivalent to that in the PZT-based piezoelectric ceramic system. The sample contains the phases $Pb(Zr_{0.525}Ti_{0.475})O_3$ *and* $Pb(Zr_{0.52}Ti_{0.48})O_3$ *with a perovskite structure, where the Zr/Ti ratios (~0.525/0.475 and 0.52/0.48) correspond to the morphotropic phase boundary (MPB). Raman spectra reveal the coexistence of orthorhombic, tetragonal, and monoclinic phases, which ensures optimal piezoelectric properties. Based on these research results, a fabrication technology using the solid-state reaction method is oriented and proposed.*

Keywords: Piezoelectric ceramics; Sonar complex MGK-400EM; OCT 11 0444-87.

1. INTRODUCTION

The 1H antenna is one of the main receiving antennas of the MGK-400EM sonar system. It is used to receive signals in the operating modes П1, A1, П2, and A3 within the frequency range of 0.3 to 10.8 kHz, serving the purposes of detection, warning, tracking, and identification of underwater targets to ensure combat readiness. The antenna is installed at the ship's bow, inside the acoustically transparent sonar dome, and has the shape of a truncated cone with its apex pointing downward at an apex angle of 12.4°. The cone has a height of about 2.4 m and a top cross-sectional diameter of 4 m. On the conical surface of the 1H antenna, 14 horizontal rings of transducer elements are arranged, each ring consisting of 72 ПР2Р transducer blocks evenly distributed around the circumference at angular intervals of 5°. Each ПР2Р transducer block is constructed from a receiving unit (ПР1 block) and an acoustic baffle [1].

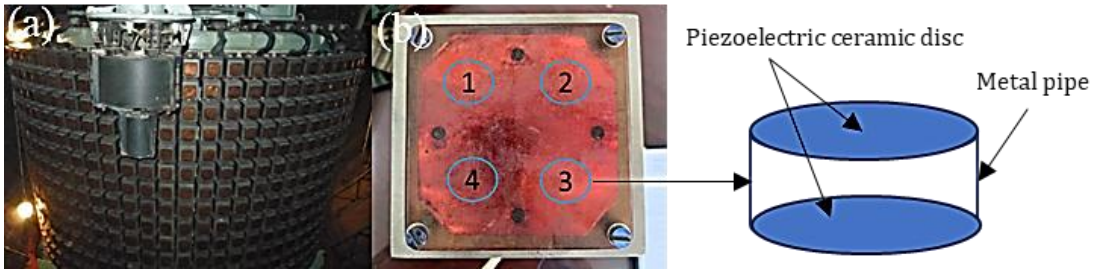

Figure 1. *(a) The 1H antenna, the receiver – ПР1 block; (b) The location of the piezoelectric ceramic [1].*

In the composition of the receiver – ПР1 block, there are four curved circular transducer units. These transducers are designed in a drum-like shape, with both faces made of piezoelectric ceramic plates (figure 1). Through these ceramic plates, acoustic signals are converted into electrical signals.

The piezoelectric ceramic plates in the transducer are manufactured according to Russian standards. Based on the available user manuals, they are identified as ЦТБС-3 ceramics, i.e., a piezoelectric ceramic system based on Pb, Ba, Zr, and Ti (PZT system). Worldwide, studies have been published on the research and development of piezoelectric transducers, taking into account thermal stresses in the design components, as well as the manufacturability and performance of sonar transducer devices based on this piezoelectric ceramic system [2]. The piezoelectric ceramics in this transducer have been in use for more than 10 years since being transferred to us, and signs of degradation requiring replacement have already appeared. These products were entirely transferred, meaning that information regarding the composition, materials, and technical specifications of the piezoelectric ceramic plates has not been disclosed. Moreover, no commercial products are available, and no domestic research or production facility has yet been able to meet the required standards. Therefore, the study on the composition, microstructure, material properties, and technological orientation for fabricating the piezoelectric ceramics used in this transducer is both highly necessary and of significant scientific and practical importance.

2. EXPERIMENTAL

2.1. Sample preparation

The piezoelectric ceramic plate currently in use has a disk shape, with both surfaces coated with a bright metallic layer. The specifications of the sample are given in table 1.

Table 1. *Shape and dimensions of the piezoelectric ceramic sample.*

Sample	Diameter, mm	Thickness, mm	Weight, g
	30 ± 1	1 ± 0,1	5,012 ± 0,001

The ceramic substrate sample used for the study was prepared by grinding to remove the metallic coating, followed by examination to determine its composition and phase structure. The composition and microstructure of the coating layer were analyzed directly on the surface, while the coating thickness was determined from the sample cross-section.

2.2. Experimental equipment

The apparent density was measured using a Shangping JA 1023 electronic balance. The microstructure, coating thickness, and chemical composition of both the coating and the ceramic substrate were examined using a JEOL JED-2300 scanning electron microscope. Phase composition was determined by X-ray diffraction (SIEMENS D5005), and phase structure was analyzed by Raman spectroscopy.

3. RESULTS AND DISCUSSION

3.1. Density of the piezoelectric ceramic sample

The density of the ceramic sample was determined using the formula [3]:

$$\rho = \frac{m_0}{(m_0 - m_1)} \times \rho_{H_2O} \left(\frac{g}{cm^3}\right) \quad (1)$$

Where: m_0 - Mass of the ceramic sample measured in air, g;

m_1 - Mass of the ceramic sample measured in water, g.

The measured density of the piezoelectric ceramic sample currently in use is ρ = 7,378 g/cm^3. From this density result, it can be observed that the Russian piezoelectric ceramic sample exhibits a significantly higher density compared to lead-free piezoelectric ceramic systems, as specified in

the industry standard OCT 11 0444-87, such as Bari titanat (TB-1) - 5.3 g/cm^3, Barium calcium titanate (TBK-3) - 5.4, Narium bismuth titanate THaB-1) - 6.80 g/cm^3 [4]. Therefore, it can be concluded that this piezoelectric ceramic is lead-based, on the basis of a PZT system, since the high density of lead (11.3 g/cm^3) contributes to the relatively high density of this ceramic system.

3.2. Microstructural characterization of the ceramic substrate and coating

The microstructure of the sample was examined on cross-sectional images, including the ceramic matrix, the coating, and the coating thickness, using a scanning electron microscope (SEM), as shown in figure 2. From figure 2(a, b), it can be observed that the piezoelectric ceramic consists of a ceramic matrix and clearly distinguishable coating layers on both surfaces, with an average coating thickness of 17.07 μm. Figure 2(c, d) present SEM images of the ceramic matrix, showing that the microstructure is composed of fine, equiaxed grains with an average size of ~ 5 μm and uniform distribution. These results are consistent with previously published studies on the microstructure of PZT-based piezoelectric ceramics fabricated by the solid-state reaction method [5-7].

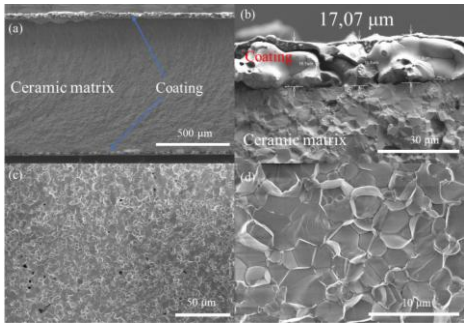

Figure 2. *SEM image of the piezoelectric ceramic sample*
(a) Sample cross-section; (b) The coating; (c), (d) SEM images of the ceramic matrix at ×600 and ×5000 magnifications, respectively.

In figure 2(c, d) at × 600 and ×5000 magnification, the ceramic matrix can be generally observed to consist of grains and grain boundaries. In addition, the appearance of black pores can be seen, which may result from the high-temperature firing process used to remove binders and during sintering in ceramic fabrication. This is also a typical characteristic of ceramics produced by this method.

3.3. Investigation of material composition and phase structure

3.3.1. Investigation of the chemical composition and phase structure of the surface coating

The investigation of the coating composition using the wide-area EDX scanning method yielded the results shown in figure 3(a), while the phase structure was determined by the XRD method, figure 3(b).

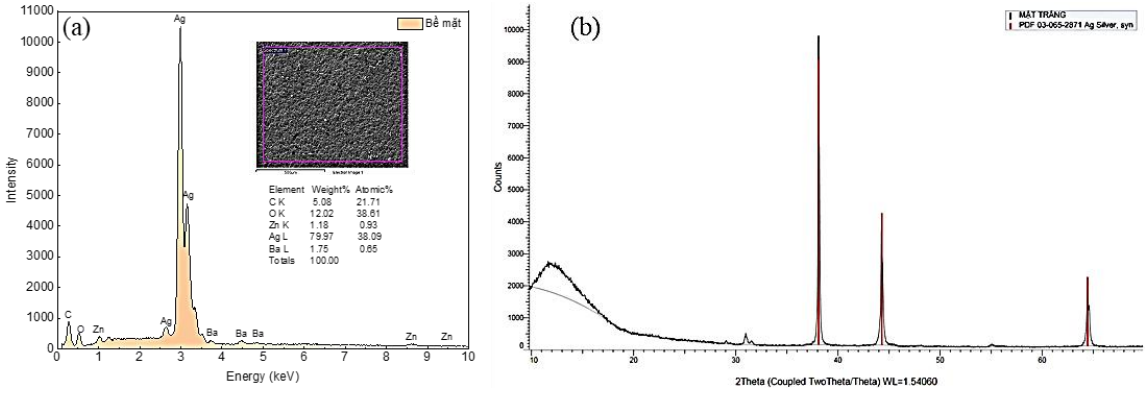

Figure 3. *(a) EDX spectrum; (b) XRD spectrum of the surface coating.*

The EDX spectra show prominent peaks at 2.634, 2.806, 2.984, and 3.151 keV, which are characteristic of silver. The silver coating is clearly present, exhibiting very strong intensity in the 2.6-3.2 keV range, corresponding to Ag's signature peaks. Other elements, such as Zn, Ba, O, and C, appear at moderate or low levels, likely due to contamination during assembly, adhesive bonding to other components of the energy transducer, or from oxides or carbon residues. The presence of Ba at 1.75% is probably attributable to the ceramic substrate.

In the XRD pattern of the Ag coating, figure 3(b), diffraction peaks are observed at 2θ angles of 38.269°, 44.44°, and 64.58°, corresponding to the crystal planes with Miller indices (hkl) of (111), (200), and (220), respectively. These results indicate that the coating is crystalline silver, consistent with the standard JCPDS card 65-2871 [8], no peaks corresponding to any secondary crystalline phases were observed. Based on the analysis of the outer coating in terms of microstructure, composition, and phase structure, it can be concluded that both surfaces of the ceramic disc are uniformly coated with a silver layer, serving as the electrodes, with a thickness of 17.07 μm.

3.3.2. Investigation of the chemical composition and phase structure of the ceramic matrix

To evaluate the uniformity of the sample composition, the authors conducted chemical analysis using EDX mapping on the cross-sectional surface of the sample. The measurement area, spectra, and elemental contents are presented in figure 4. The EDX results and corresponding maps indicate a uniform distribution of Zr, O, Pb, Sr, Ti, and Ba within the analyzed region (figure 4(b-g)), suggesting that the fabrication process of the piezoelectric ceramic was carried out homogeneously.

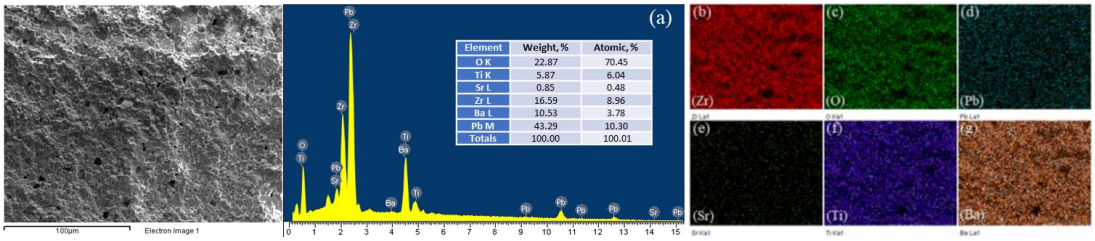

Figure 4. *(a) EDX spectrum and elemental mapping of the sample; Distribution maps of (b) zirconium, (c) oxygen, (d) lead, (e) strontium, (f) titanium, and (g) barium at a magnification of 500×.*

The chart in figure 4(a) shows characteristic peaks corresponding to the elemental composition of the ceramic. These are the main elements in the ceramic sample, appearing with multiple occurrences and characteristic intensities typical of the ЦТБС piezoelectric system, consistent with previously reported EDS studies on piezoelectric ceramics [6]. Strontium is present in the sample at a relatively low concentration, with an average value of 0.85%. It is likely a dopant introduced into the ceramic system to enhance the piezoelectric properties, as well as to improve the temperature stability and mechanical strength of the ceramic [4]. The survey results for the average composition (% by weight and molar fraction) from three measurements are as follows: Pb 43.29 wt% (0.209 mol), Ba 10.53 wt% (0.077 mol), Zr 16.59 wt% (0.182 mol), Ti 5.87 wt% (0.123 mol), O 22.87 wt% (1.429 mol), and Sr 0.85 wt% (0.01 mol). To approximate the perovskite ABO_3 formula, the A-site occupancy is calculated as Pb = 0.209 /(0.209+0.077) = 0.731 and Ba = 0.269. For the B-site, Zr = 0.182/(0.182+0.123) = 0.597 and Ti = 0.403. Thus, the approximate formula based on the EDS analysis results is $Pb_{0.731}Ba_{0.269}(Zr_{0.597}Ti_{0.403})O_3$. Based on this calculation, the Zr/Ti ratio of 0.597/0.403 corresponds to a composition near the morphotropic phase boundary (MPB), which leads to enhanced domain structure and improved piezoelectric performance [9]. However, the calculated formula may still contain measurement errors, and during the fabrication process, some elements-particularly Pb, as well as Ba and O-may volatilize.

The XRD pattern of the piezoelectric ceramic sample was measured over a 2θ range of 10° to 80°, using X-ray radiation with a wavelength of λ = 1.54060 Å, as shown in figure 5(a).

The XRD pattern of the ceramic sample, compared with the standard reference cards PDF 201-070-0743 and COD2102948 from reference [6] shows peaks at 2θ values of 22.02°, 30.97°, 38.27°, 44.05°, 50.63°, 55.99°, 64.81°, 68.92°, and 73.54°, corresponding to the crystal planes (001), (011), (111), (002), (012), (112), (220), (211), and (130), respectively. The presence of these peaks, when compared with the Pb(Zr,Ti)O_3 ceramic substrate and standard reference cards, indicates that they are equivalent. The observed peaks correspond to the coexistence of two phases in the microstructure: a rhombohedral phase (R3c) and a cubic phase (Pm-3m) [6]. The XRD results shown in figure 5(a), combined with the standard reference cards PDF 01-072-7170 and PDF 01-070-4060, also indicate the presence of an additional phase $Pb(Zr_{0.525}Ti_{0.475})O_3$, $Pb(Zr_{0.52}Ti_{0.48})O_3$, PDF 01-082-2643 the presence of the phase $Pb_{0.7}Ba_{0.3}(Zr_{0.4}Ti_{0.6})O_3$ The presence of these phases indicates that the piezoelectric ceramic sample is based on the ЦТБС system. The XRD results show that the main phase of the ceramic substrate is PZT, with a Zr/Ti ratio of 0.525/0.475 or 0.52/0.48. With this crystal structure, it can be seen that the fabricated piezoelectric ceramic has its main composition located at the morphotropic phase boundary (MPB) of the PZT system, where the piezoelectric and dielectric properties are optimized [10]. The substitution of Ba^{2+} for Pb^{2+} at the A-site of the perovskite ABO_3 lattice, with a Pb/Ba ratio of 7/3, reduces the sintering temperature and increases grain boundary mobility [11].

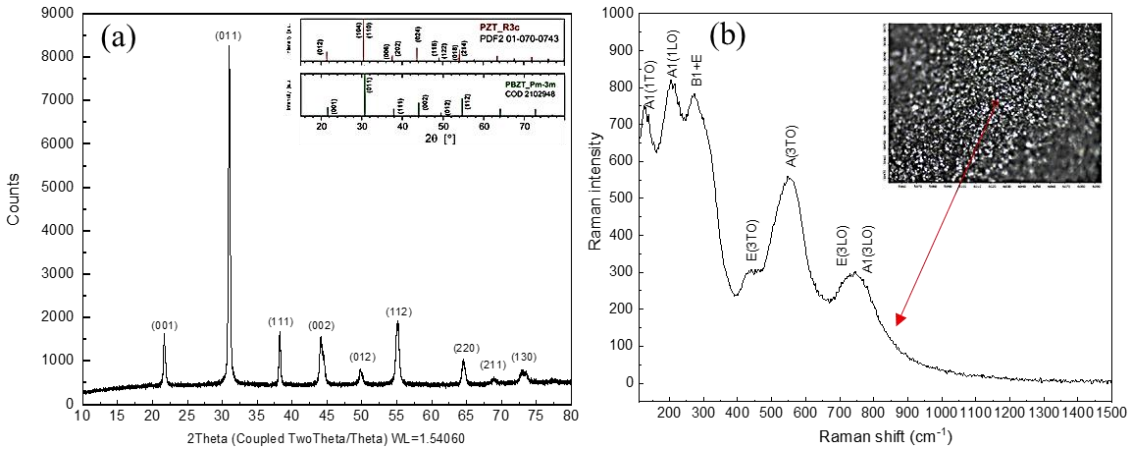

Figure 5. *(a) XRD spectrum; (b) Raman spectrum of the piezoelectric ceramic matrix.*

The Raman spectrum analysis shown in figure 5(b) exhibits several characteristic peaks of the PZT-based piezoelectric ceramic, including: 126.22 cm^{-1}→A_1(1TO), characteristic of the tetragonal phase of the substrate; 204.13 cm^{-1}→E(2TO); 272.78 cm^{-1}→B_1 + E, indicative of the tetragonal/rhombohedral phase, representing the two phases at the MPB; 547.52 cm^{-1}→E(3TO), showing the presence of both monoclinic and tetragonal phases; and 746.21 cm^{-1}→E(3LO) + A_1(3LO), characteristic of the tetragonal structure [10]. From this investigation, it can be observed that, in addition to the characteristic peaks of the PZT ceramic substrate with tetragonal and rhombohedral phases, the spectrum also shows peaks indicating the presence of the morphotropic phase boundary (MPB) and the coexistence of multiple phases, including the monoclinic phase. The presence of the monoclinic phase is one of the factors contributing to the excellent piezoelectric properties of this ceramic system [12].

3.4. Fabrication process orientation

Piezoelectric ceramics are currently used in energy transducers. Based on the compositional analysis above, the ceramic system is equivalent to the ЦТБС system. This is a ЦТБС-based ceramic with the addition of Ba, which reduces the Pb content during fabrication, thereby decreasing environmental toxicity while still maintaining piezoelectric properties. Furthermore, the substitution of Ba^{2+} and Sr^{2+} at the A-site represents an isovalent cation replacement in the perovskite lattice,

which helps to adjust the crystal structure and the piezoelectric–dielectric properties of the material. The fabrication process is guided through 12 steps, as illustrated in figure 6.

The fabrication process includes the following steps: (1) Raw materials: PbO (≥ 99.9%), TiO_2-rutile (≥ 99.5%), ZrO_2-tetragonal (≥ 99.9%), $BaCO_3$ (≥ 99.95%), and small amounts of dopants such as $SrCO_3$ (≥ 99.95%) are accurately measured; (2) Mixing: The raw materials are thoroughly mixed and finely milled to ensure homogeneity; (3) Calcining: A high-temperature solid-state reaction is conducted to form the ceramic structure, which is critical for the final product performance; (4) Milling: Further milling is performed to improve the uniformity and performance consistency; (5) Granulation: Granules with high density and good flowability are produced; (6) Pressing: The granules are pressed to form green bodies with the desired dimensions; (7) Binder Removal: Organic binders used during granulation are removed; (8) Sintering: The green bodies are sintered to densify the ceramic; (9) Grinding/polishing: Final shaping and dimension adjustments are carried out; (10) Electroding: Electrodes are applied onto the ceramic surfaces; (11) Poling: Electric domains are oriented to induce piezoelectric properties; (12) Final inspection: The final ceramic is tested for its electrical and piezoelectric properties.

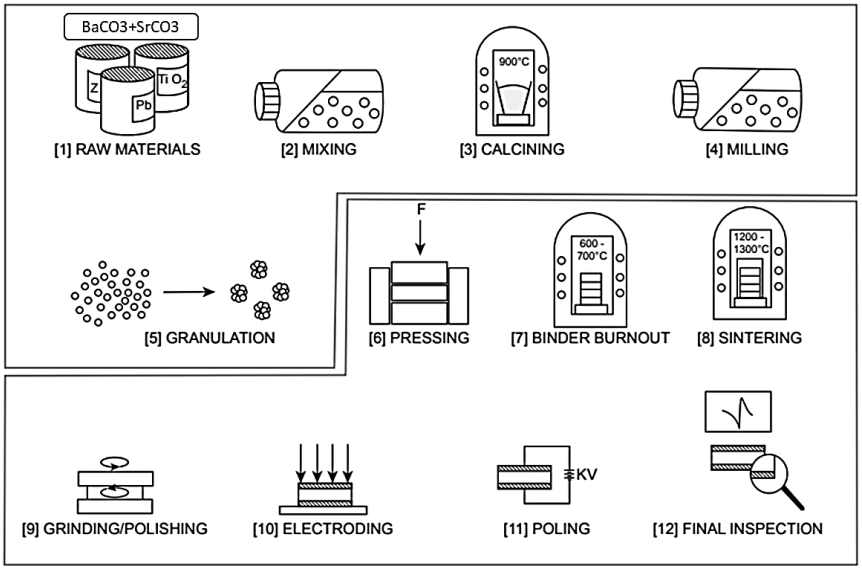

Figure 6. *Schematic diagram of the guided fabrication process of piezoelectric ceramics.*

4. CONCLUSIONS

In this study, several analyses indicate that the piezoelectric ceramic used is a lead-based ceramic, with a bulk density of 7.378 g/cm³. Both surfaces of the disc are coated with silver, with an average coating thickness of 17.07 μm. The ceramic substrate consists of small, uniform grains with an average size of ~5 μm. The composition of the piezoelectric ceramic, in terms of average mass fraction, includes 43.29% Pb, 10.53% Ba, 16.59% Zr, 5.87% Ti, 22.87% O, and 0.85% Sr, with Sr acting as a minor dopant equivalent to the ЦТБС system. The ceramic contains phases of $Pb(Zr_{0.525}Ti_{0.475})O_3$ and $Pb(Zr_{0.52}Ti_{0.48})O_3$, corresponding to compositions at the morphotropic phase boundary (MPB) of the ЦТБС piezoelectric system, where the piezoelectric and dielectric properties are optimized. Based on these material investigations, the research team proposed a 12-step solid-state synthesis process for fabricating the piezoelectric ceramic discs. These results constitute the initial findings, providing a foundation for further studies aimed at mastering the fabrication technology of this ceramic system.

Acknowledgment: *The authors gratefully acknowledge the financial support provided by the Institute of Science and Technology of the Military, under the 2025 scientific research project.*

REFERENCES

[1]. Naval Technical Department, *"Hướng dẫn sử dụng tổ hợp sonar MGK-400EM, Phần 1 Thuyết minh hướng dẫn sử dụng",* (2012) (in Vietnamese).

[2]. Михаил Валерьевич Богуш, Ольга Михайловна Богуш, Эдуард Михайлович Пикалев, *"Анализ температурных напряжений в элементах гидроакустических антенн (Thermal stresses analysis in the elements of sonar antenna)"*, Приборы, 10, 38–42, (2013).

[3]. Tran Van Quynh et al., *"Công nghệ vật liệu điện tử",* Science and Technology Publishing House, (2006) (in Vietnamese).

[4]. ОСТ 11 0444-87, *"Материалы пьезокерамические"*, Технические условия, (1987).

[5]. Топчиев Анатолий Андреевич, *"Влияние модификаторов на диэлектрические свойства и формирование структуры керамики на основе цирконата-титаната свинца"*, Диссертация кандидата физико-математических наук, (2021).

[6]. Małgorzata Adamczyk-Habrajska et al., *"Impedance Spectroscopy of Lanthanum-Doped (Pb0.75Ba0.25)(Zr0.7Ti0.3)O3 Ceramics"*, Applied Sciences, 14(21), 9854, (2024).

[7]. Chakkaphan Wattanawikkam et al., *"Crystal structure and microstructure of (Pb1−xBax)(Zr1−yTiy)O3 ceramics prepared by the solid state reaction method"*, Ferroelectrics, 403(1), 166–174, (2010).

[8]. R. Kalaivani et al., *"Synthesis of chitosan mediated silver nanoparticles (Ag NPs) for potential antimicrobial applications"*, Frontiers in Laboratory Medicine, 2(1), 30–35, (2018).

[9]. W. R. Jaffe et al., *"Piezoelectric Ceramics"*, Academic Press, New York, (1971).

[10]. Amid Shakeri et al., *"An investigation of solvent effect on rhombohedral/monoclinic/tetragonal phase properties of Pb(Zr0.53Ti0.47)O3 nanoparticles prepared via sol-gel method"*, Advanced Materials Research, 829, 698–702, (2014).

[11]. Mirta Mir et al., *"X-ray powder diffraction structural characterization of Pb1−xBaxZr0.65Ti0.35O3 ceramic"*, Structural Science, 63(5), 713–718, (2007).

[12]. B. Noheda et al., *"Stability of the monoclinic phase in the ferroelectric perovskite PbZr1−xTixO3"*, Physical Review B, 63(1), 014103, (2000).

TÓM TẮT

Nghiên cứu khảo sát thành phần, tổ chức và định hướng công nghệ chế tạo gốm áp điện sử dụng trong bộ biến năng đặc chủng lĩnh vực thủy âm

Bài báo trình bày một số kết quả nghiên cứu về thành phần và tổ chức của gốm áp điện hiện đang được sử dụng trong các bộ biến năng. Trên cơ sở đó, định hướng công nghệ chế tạo gốm áp điện dạng đĩa cho anten 1H của hệ thống sonar MGK-400EM. Kết quả cho thấy gốm áp điện có nền chì, với khối lượng riêng là 7,378 g/cm³, hai bề mặt đều được phủ Ag, với độ dày trung bình là 17,07 µm. Nền gốm bao gồm các hạt mịn, đồng đều với kích thước trung bình 5 µm. Kết quả phân tích EDX cho thấy nguyên tố chính phân bố đồng đều theo khối lượng là 43,29% Pb, 10,53% Ba, 16,59% Zr, 5,87% Ti, 22,87% O và 0,85% Sr, trong đó Sr đóng vai trò là chất pha tạp tương đương với hệ gốm áp điện PZT. Mẫu chứa các pha $Pb(Zr_{0.525}Ti_{0.475})O_3$ *và* $Pb(Zr_{0.52}Ti_{0.48})O_3$ *với cấu trúc perovskite, trong đó tỷ lệ Zr/Ti (~0,525/0,475 và 0,52/0,48) tương ứng với ranh giới pha hình thái (MPB). Phổ Raman cho thấy sự đồng tồn tại của các pha trực thoi, tứ giác và đơn tà, đảm bảo các tính chất áp điện tối ưu. Dựa trên những kết quả nghiên cứu này, một công nghệ chế tạo sử dụng phương pháp phản ứng thể rắn được định hướng đề xuất.*

Từ khóa: Gốm áp điện; Tổ hợp sonar MGK-400EM; ОСТ 11 0444-87.